When Quasistatic Jamming is Impossible *

J.C. Trinkle S.L. Yeap L. Han

Department of Computer Science
Texas A&M University
College Station, TX 77843-3112

Abstract

We propose a new condition to test for the impossibility of jamming in three-dimensional, quasistatic multi-rigid-body systems. Our condition can be written as a feasibility problem for a system of linear inequalities and therefore can be checked using linear programming techniques. To demonstrate the use of our jamming test, we apply it to a simple dexterous manipulation task and to the well-known peg-in-hole insertion problem.

1 Introduction

To plan successful parts-mating operations, one must be able to determine whether a candidate plan or plan segment is prone to jamming. In this paper, we develop sufficient conditions for the *impossibility* of jamming. The basic idea is simple. We consider a compliant manipulation task with one or more sliding contacts. Then we consider the possibility that one or more sliding contacts converts to rolling. If this were to occur, the position-controlled joints could not follow their planned trajectories, and efforts associated with position errors would accrue. As the errors build, the converted contacts would either continue to roll (sustaining the jam) or convert back to sliding. Here we assume that the jam will be sustained if, in order to resist the building control forces, the contact force of at least one contact has to move strictly inside its friction cone. Otherwise, we assume that a sustained jam is impossible.

*This research was supported in part by the National Science Foundation, grant no. IRI-9304734, the Texas Advanced Research Program, grant no. 999903-078, and the Texas Advanced Technology Program, grant no. 999903-095. Any findings, conclusions, or recommendations expressed herein are those of the authors and do not necessarily reflect the views of the granting agencies.

2 Previous Work

Jamming must be well understood before reliable automatic manipulation and assembly planners can be developed. However, progress has been slow for general systems. Several authors have studied the jamming of (nominally) rigid parts, but this has been done mostly for special geometries, such as a peg and a hole (see [1, 8, 12]).

Donald and Pai [3], and later Dupont [4] developed jamming analyses for systems with more general geometries. Donald and Pai's work grew out of the development of a simulator designed to test plans for assembling compliant parts. Compliant bodies were approximated by connecting rigid parts with torsion springs. They assumed Coulomb friction acted at the contacts and that dynamic effects were negligible. In order to simulate the assembly of such parts, they developed a technique to predict jamming. Dupont's work was more general. He also assumed dry friction acted at the contacts, but his analysis was for three-dimensional bodies and he included dynamic effects.

Our analysis of jamming applies to arbitrary quasistatic, three-dimensional, multi-rigid-body systems and allows for a subset of the joints to operate under compliant control. We use the knowledge of the planned joint trajectories and the errors that would be induced by jamming to develop mathematical conditions for which jamming is *impossible*.

3 Assumptions

Our basic assumptions are that the bodies are rigid, the joints of the manipulator can be position- or effort-controlled as desired, [1] and Coulomb friction acts at the contact points. Further, we will assume that the conditions of first-order stability with friction [9] are met by the manipulation plan. First-order stability

[1] By effort-controlled, we mean that a prismatic joint is force-controlled and a revolute joint is torque-controlled.

implies that a contact mode has been chosen and the joints of the manipulator have been partitioned into position- and effort-controlled subsets to guarantee that:

1. The velocities of the position-controlled joints uniquely determine the velocities of the effort-controlled joints and the manipulated object.
2. The contact forces (for the planned contact mode) and the efforts of the position-controlled joints can be determined uniquely from the externally applied forces and the efforts of the effort-controlled joints.
3. The contact forces at the rolling contacts lie strictly within their respective friction cones.

Note that if a manipulation system maintains first-order stability along its planned trajectory, then rolling contacts will continue to roll and no contact will separate in response to small disturbing forces. However, as alluded to in the "Introduction," it is possible for a sliding contact to convert to rolling, because Coulomb's Law is ambiguous with regard to sliding and rolling when a contact force lies on the boundary of its friction cone. When a sliding contact *does* switch to rolling, it imposes kinematic constraints on the system that are, in general, inconsistent with the planned control modes of the joints. For this reason, we refer to the system as jammed whenever a sliding contact converts to rolling. Kinematic inconsistency also occurs when a new contact is unexpectedly formed, but that case will not be considered, because such events can be predicted during planning and the appropriate change in the control mode partition can be easily determined.

4 Formulation of Jamming Condition

We assume that a first-order stable manipulation plan with at least one sliding contact has been provided. Our objective here is to determine whether or not jamming is possible at a given configuration along the planned trajectory.

Since the contact mode is known and the plan is first-order stable, we can write the applicable kinematic constraints for any point on the manipulation trajectory. Let $\dot{\boldsymbol{q}} \in \mathcal{R}^6$ and $\dot{\boldsymbol{\theta}} \in \mathcal{R}^{n_\theta}$, be the generalized velocity vectors of the workpiece and manipulator, respectively, where $\mathcal{R}^n$ denotes n-dimensional Euclidean space. Then the kinematic velocity constraint implied by the planned contact mode is [11]:

$$\boldsymbol{W}_A^T \dot{\boldsymbol{q}} - \boldsymbol{J}_A \dot{\boldsymbol{\theta}} = \boldsymbol{0} \qquad (1)$$

where the matrices $\boldsymbol{W}_A^T$ and $\boldsymbol{J}_A^T$ have three rows for each rolling contact and one row for each sliding contact (*i.e.*, $3n_R + n_S$, where n_R and n_S are the numbers of rolling and sliding contacts respectively). These matrices are partitions of the Jacobian of the positional kinematic constraints associated with the contacts constraints.

At each sliding contact, the direction of the friction force is known and proportional to the normal reaction. Thus we can write the equilibrium equations as [9]:

$$\begin{bmatrix} \boldsymbol{W}_{A\mu} \\ \boldsymbol{J}_{A\mu}^T \end{bmatrix} \boldsymbol{c}_A = \begin{bmatrix} -\boldsymbol{g}_{obj} \\ \boldsymbol{\tau} - \boldsymbol{g}_{man} \end{bmatrix}. \qquad (2)$$

where the unknown $\boldsymbol{c}_A$ is referred to as the applicable wrench intensity vector. This vector contains three wrench intensities for each rolling contact, and one wrench intensity for each sliding contact. Note that the dimension of $\boldsymbol{W}_{A\mu}$ is the same as that of $\boldsymbol{W}_A$ and their columns corresponding to the rolling contacts are identical. However, the columns of $\boldsymbol{W}_{A\mu}$ corresponding to the sliding contacts are wrenches corresponding to contact forces on the boundaries of the friction cones (*e.g.*, $\boldsymbol{w}_{ix}$ in Figure 1), while those in $\boldsymbol{W}_A$ correspond to the normal directions at the sliding contacts (*e.g.*, $\boldsymbol{w}_{in}$ in Figure 1). The matrices $\boldsymbol{J}_{A\mu}$ and $\boldsymbol{J}_A$ are similarly related.

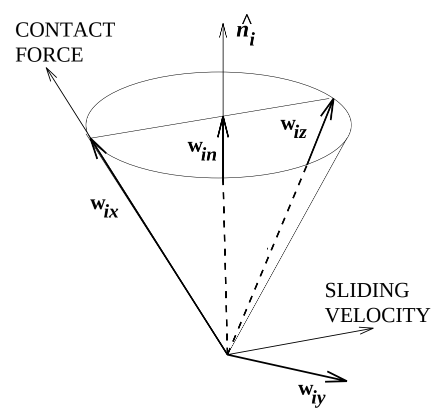

Figure 1: The Friction Cone and Wrench Basis

Now we are in a position to derive conditions under which jamming is not sustainable. Consider a situation in which only contact i is sliding. The system will jam if the i^{th} contact force moves inside its friction cone. To test for this possibility, we reformulate the equilibrium equations with additional wrench intensities for the sliding contact as follows:

$$\left[\begin{array}{ccc} \boldsymbol{W}_{A\mu} & \boldsymbol{w}_{iy} & \boldsymbol{w}_{iz} \\ \boldsymbol{J}_{A\mu}^T & \boldsymbol{j}_{iy}^T & \boldsymbol{j}_{iz}^T \end{array} \right] \left[\begin{array}{c} \boldsymbol{c}_A \\ c_{iy} \\ c_{iz} \end{array} \right] = \left[\begin{array}{c} -\boldsymbol{g}_{obj} \\ \boldsymbol{\tau} - \boldsymbol{g}_{man} \end{array} \right] \quad (3)$$

where the vectors, $\boldsymbol{j}_{iy}^T$ and $\boldsymbol{j}_{iz}^T$, are the columns of the Jacobian matrix corresponding to the unit wrenches, $\boldsymbol{w}_{iy}$ and $\boldsymbol{w}_{iz}$ (shown in Figure 1). Note that if the contact continues to slide, the new wrench intensities, c_{iy} and c_{iz}, will be zero. Jamming cannot be sustained if eq. (3) cannot be satisfied with $c_{iz} > 0$.

Since the trajectory under consideration is first-order stable, the matrix in the equilibrium equations can be partitioned to yield (see [9] for details):

$$\left[\begin{array}{ccc} \boldsymbol{Q}_I & \boldsymbol{y}_{iI} & \boldsymbol{z}_{iI} \\ \boldsymbol{Q}_{II} & \boldsymbol{y}_{iII} & \boldsymbol{z}_{iII} \end{array} \right] \left[\begin{array}{c} \boldsymbol{c}_A \\ c_{iy} \\ c_{iz} \end{array} \right] = \left[\begin{array}{c} \boldsymbol{g}_I \\ \boldsymbol{\tau}_{II} - \boldsymbol{g}_{manII} \end{array} \right], \quad (4)$$

where $\boldsymbol{Q}_I^{-1}$ exists (the structure of $\boldsymbol{g}_I$ will be revealed in the next equation). The vector of efforts at the position-controlled joints, $\boldsymbol{\tau}_{II}$, can now be written as a function of the efforts at the other joints, $\boldsymbol{\tau}_I$:

$$\begin{aligned} \boldsymbol{\tau}_{II} &= \boldsymbol{Q}_{II}\boldsymbol{Q}_I^{-1} \left[\begin{array}{c} -\boldsymbol{g}_{obj} \\ \boldsymbol{\tau}_I - \boldsymbol{g}_{manI} \end{array} \right] + \boldsymbol{g}_{manII} \\ &+ (\boldsymbol{y}_{iII} - \boldsymbol{Q}_{II}\boldsymbol{Q}_I^{-1}\boldsymbol{y}_{iI})c_{iy} \\ &+ (\boldsymbol{z}_{iII} - \boldsymbol{Q}_{II}\boldsymbol{Q}_I^{-1}\boldsymbol{z}_{iI})c_{iz}. \end{aligned} \quad (5)$$

Note that when $c_{iy} = c_{iz} = 0$, $\boldsymbol{\tau}_{II}$ takes on its value just prior to jamming. This implies that the third and fourth terms of the right hand side of eq. (5) represent the changes in the efforts, $\Delta\boldsymbol{\tau}_{II}$, of the position-controlled joints caused by the jam.

The last step in the analysis is to determine the jam-induced changes in the joint torques and relate them to the new wrench intensities. Of the position controlled joints, a subset of those will jam if one or more of the sliding contacts convert to rolling. Let $\boldsymbol{E}_J$ be the matrix of zeros and ones that selects the jammed joint from the position-controlled joints. Specifically, premultiplying $\Delta\boldsymbol{\tau}_{II}$, by $\boldsymbol{E}_J$ removes the elements corresponding to the joints that do *not* jam. Finally, denote by $\boldsymbol{X}$, the diagonal matrix with i^{th} diagonal entry given by the sign of the accrued position error at the i^{th} jammed joint. Then for the changes in the joint efforts to be consistent (in sign) with their positional errors, we have:

$$\boldsymbol{X}\boldsymbol{E}_J \Delta\boldsymbol{\tau}_{II} > \boldsymbol{0}. \quad (6)$$

Note that it is possible that inequality (6) be satisfied by equality only if the conversion of sliding to rolling happens to generate constraints that do not make the kinematic velocity constraints (1) inconsistent. Since this situation is rare, we will not consider the possibility further.

Substituting the third and fourth terms on the right hand side of eq. (5) into inequality (6) yields the conditions for *possible* jamming (*i.e.*, the following are necessary conditions for jamming):

$$\boldsymbol{X}\boldsymbol{E}_J \left[\begin{array}{c} (\boldsymbol{y}_{iII} - \boldsymbol{Q}_{II}\boldsymbol{Q}_I^{-1}\boldsymbol{y}_{iI})^T \\ (\boldsymbol{z}_{iII} - \boldsymbol{Q}_{II}\boldsymbol{Q}_I^{-1}\boldsymbol{z}_{iI})^T \end{array} \right]^T \left[\begin{array}{c} c_{iy} \\ c_{iz} \end{array} \right] > 0 \quad (7)$$

$$c_{iz} \geq 0 \quad (8)$$

We stress that satisfaction of the system (7) and (8) implies that the situation is "ripe" for jamming. If a conversion from sliding to rolling occurs, then c_{iz} can increase driving the contact force inside the friction cone, thus sustaining the jam. However, if the system of inequalities is not feasible, then contact i cannot convert to rolling, because the changes in the joint efforts corresponding to the change in the i^{th} contact force are not consistent with the joint position errors.

Note that constraints on c_{iy} forcing it to be consistent with Coulomb's Law are *not* included here. This is because we are interested in the infeasibility of system (7) and (8). In particular, if the system (7) and (8) is infeasible, then it is still infeasible if additional constraints are imposed. One could justify the inclusion of constraints on c_{iy} on the grounds that our test (for the impossibility of jamming) would then be less conservative, but we do not include them here.

Extending the possible jamming conditions, inequalities (7) and (8), to situations with more than one sliding contact leads to:

$$\boldsymbol{X}\boldsymbol{E}_J \left[\begin{array}{c} (\boldsymbol{Y}_{II} - \boldsymbol{Q}_{II}\boldsymbol{Q}_I^{-1}\boldsymbol{Y}_I)^T \\ (\boldsymbol{Z}_{II} - \boldsymbol{Q}_{II}\boldsymbol{Q}_I^{-1}\boldsymbol{Z}_I)^T \end{array} \right]^T \left[\begin{array}{c} \boldsymbol{c}_y \\ \boldsymbol{c}_z \end{array} \right] > \boldsymbol{0} \quad (9)$$

$$\boldsymbol{c}_z \geq \boldsymbol{0} \quad (10)$$

where the matrices $\boldsymbol{Y}_I$, $\boldsymbol{Y}_{II}$, $\boldsymbol{Z}_I$, and $\boldsymbol{Z}_{II}$ are formed by horizontally concatenating n_S vectors $\boldsymbol{y}_{iI}$, $\boldsymbol{y}_{iII}$, $\boldsymbol{z}_{iI}$, and $\boldsymbol{z}_{iII}$ for the sliding contacts. The product of the matrices appearing in ineq.(9), is referred to as the *jamming matrix*. The numbers of rows of the matrices subscripted by I and II are $3n_R + n_S$ and $6 + n_\theta - 3n_R - n_S$, respectively, so the numbers of rows and columns in the jamming matrix are the number of position-controlled joints, $6 + n_\theta - 3n_R - n_S$, and twice the number of sliding contacts, $2n_S$, respectively.

The above development is summarized by the following theorem and corollary.

Theorem 1 *An active, three-dimensional, multi-rigid-body system with Coulomb friction acting at the contacts cannot jam if the system of inequalities (9) and (10) is infeasible.*

Proof: See [9] for a proof.

Corollary 1 *An active, two-dimensional, multi-rigid-body system with Coulomb friction acting at the contacts cannot jam if any row of the matrix,* $\boldsymbol{X}\boldsymbol{E}_J(\boldsymbol{Z}_{II} - \boldsymbol{Q}_{II}\boldsymbol{Q}_I^{-1}\boldsymbol{Z}_I)$*, has all nonpositive elements.*

Proof: In the planar case, $\boldsymbol{c}_y$ is zero by definition and the jamming matrix reduces to $\boldsymbol{X}\boldsymbol{E}_J(\boldsymbol{Z}_{II} - \boldsymbol{Q}_{II}\boldsymbol{Q}_I^{-1}\boldsymbol{Z}_I)$. Since $\boldsymbol{c}_z$ is nonnegative, if any row of the jamming matrix has all nonpositive elements, then that row dotted with $\boldsymbol{c}_z$ is clearly nonpositive, thus violating the corresponding inequality in (9). ... *q.e.d.*

4.1 Jamming Example: Block in Palm

Figure 2 shows a simple planar system in which the stick finger begins at an angle just less than $\pi/2$ and rotates clockwise under position control, pushing the block to the right along the palm. The contact mode of interest is the one maintaining the three contacts shown (the edge-edge contact is modeled as two point contacts between the palm and two corners of the block). For the commanded clockwise finger motion, this system exhibits jamming in some configurations and first-order stability in others. For simplicity,

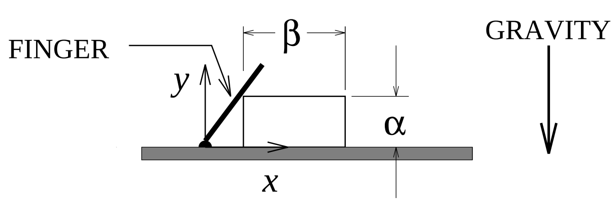

Figure 2: A Planar Manipulation System

assume that the coefficients of friction, μ_i, at the three contacts are equal. Then, given that the world frame has its origin on the axis of the revolute joint of the stick finger and the external force (in this example, the gravitational force) acts in the $-y$-direction, the relevant matrices are defined as follows:

$$\boldsymbol{W}_n = \begin{bmatrix} 0 & 0 & sin(\theta) \\ 1 & 1 & -cos(\theta) \\ x & x+\beta & -\gamma \end{bmatrix} \quad (11)$$

$$\boldsymbol{J}_n^T = \begin{bmatrix} 0 & 0 - \gamma \end{bmatrix} \quad (12)$$

$$\boldsymbol{W}_t = \begin{bmatrix} -1 & -1 & cos(\theta) \\ 0 & 0 & sin(\theta) \\ 0 & 0 & 0 \end{bmatrix} \quad (13)$$

$$\boldsymbol{J}_t^T = \begin{bmatrix} 0 & 0 & 0 \end{bmatrix} \quad (14)$$

$$\boldsymbol{Q}_I = \begin{bmatrix} -\mu & -\mu & sin(\theta) - \mu cos(\theta) \\ 1 & 1 & -cos(\theta) - \mu sin(\theta) \\ x & x+\beta & -\gamma \end{bmatrix} \quad (15)$$

$$\boldsymbol{Q}_{II} = \begin{bmatrix} 0 & 0 & -\gamma \end{bmatrix} \quad (16)$$

$$\boldsymbol{Z}_I = \begin{bmatrix} \mu & \mu & sin(\theta) + \mu cos(\theta) \\ 1 & 1 & -cos(\theta) + \mu sin(\theta) \\ x & x+\beta & -\gamma \end{bmatrix} \quad (17)$$

$$\boldsymbol{Z}_{II} = \begin{bmatrix} 0 & 0 & -\gamma \end{bmatrix} \quad (18)$$

where $\gamma = \sqrt{x^2 + \alpha^2}$. Assuming $\boldsymbol{g}_{man} = 0$, the generalized applied force is given as:

$$\begin{bmatrix} -\boldsymbol{g}_{obj} \\ \boldsymbol{\tau} - \boldsymbol{g}_{man} \end{bmatrix} = \begin{bmatrix} 0 \\ mg \\ (x + \beta/2)mg \\ \tau \end{bmatrix} \quad (19)$$

where m is the mass of the block and g is the magnitude of the gravitational acceleration.

If a contact converts to rolling while the other contacts are maintained, it is clear that motion will cease. Hence, $\boldsymbol{E}_J = 1$. Then, since the planned finger motion was clockwise rotation, the controller error will be negative, leading to $\boldsymbol{X} = -1$.

To further simply our discussion and the algebra, let $\mu = 0.5$, $\alpha = 1$ and $\beta = 2$. Maintaining the chosen contact mode allows the elimination of the finger joint angle from the quasistatic equations. Then, the applicable wrench intensity vector, $\boldsymbol{c}_A$, is given as:

$$\boldsymbol{c}_A = \begin{bmatrix} -\frac{mg(3+x)/4}{2x-3/2} \\ -\frac{5mg(1-x)/4}{2x-3/2} \\ -\frac{mg\sqrt{x^2+1}}{2x-3/2} \end{bmatrix} \quad (20)$$

and the (1×3) jamming matrix is:

$$\begin{bmatrix} \frac{2(x^2+1)}{2x-3/2} & \frac{2(x^2+1)}{2x-3/2} & \sqrt{x^2+1} + \frac{5/2\sqrt{x^2+1}}{2x-3/2} \end{bmatrix}. \quad (21)$$

Note that all three elements of $\boldsymbol{c}_A$ are positive and all the elements of the jamming matrix are negative when $0 < x < 3/4$. Thus the system is first-order stable over that open interval. As x approaches $3/4$ from the left, the elements of the jamming matrix go to negative infinity, and the elements of the wrench intensity vector, $\boldsymbol{c}_A$, and the joint torque, τ, go to positive infinity. When $x > 3/4$, all the elements of the jamming matrix are positive, so jamming is possible and first-order stability is lost. In this particularly simple example, the system must jam when x reaches $3/4$ (assuming that it begins with $x < 3/4$). One can show that no other contact mode is possible [11]. This result is intuitively appealing, since the torque goes to infinity at $x = 3/4$.

It is interesting to compare the results of the block/hand example with results on frictional form closure. One might expect that jamming will occur when the block moves into a position of frictional form closure. However, this is not the case. Observe that at the point $x = 3/4$ the active edges of the friction cones are all parallel, but that no pair of the cones (or negative cones) see each other as is required for frictional form closure [2, 10].[2] In fact, only the cone on the finger and the cone on the left side of the block can ever see each other, and this first happens as x increases beyond 2.0. However, as noted above that the system jams when x reaches $3/4$ even though form closure is *not* achieved.

In trying to reconcile the unexpected difference between jamming and form closure, we thought that perhaps we should not model the edge contact along the palm as two distinct point contacts with friction. Therefore, we used Omata's idea to replace the two friction cones on the palm by a single "equivalent" friction cone [6]). This cone has its apex 2 distance units below the center of the bottom of the block and its edges are colinear with the outer edges of the two individual friction cones. This cone and the cone on the finger do not "see each other" until $x > 1.0$. So jamming still will occur before frictional form closure is achieved by Omata's model. Our explanation for this result is that previous form closure results do not take the kinematic structure of the grasping mechanism into account, but we do here.

4.2 Jamming Example: Peg-in-Hole

The peg-in-hole insertion problem (see Figure 3) has been studied in great depth (so to speak) by [12, 8, 1]. It was found by Whitney, that the peg is most likely to jam when there are two points of contact and the insertion depth is small. We derived the jamming matrix for this compliant motion task (assuming the maintenance of two points of contact) and plotted the jamming matrix elements for a variety of clearances and coefficients of friction (possibly different at the two contacts). When the coefficients of friction were zero, so were the elements of the jamming matrix. When the coefficients were nonzero, at least one jamming matrix element was positive at the beginning of insertion. This corroborates Whitney's findings.

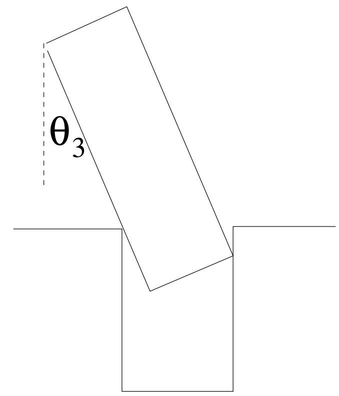

Figure 3: Peg-in-Hole Insertion

Figure 4 shows a typical plot of the elements of the jamming matrix versus the tilt angle of the peg. Insertion progresses from right to left on the abscissa, as insertion is complete when the tilt angle is zero. The extreme right of the plot corresponds to insertion beginning with the right bottom corner of the peg in contact with the right side of the hole at its top corner. Note that as insertion proceeds, the jamming matrix elements become negative, indicating that jamming becomes impossible after a certain depth of insertion. The depth at which this occurs moves rightward as the coefficient of friction decreases.

5 Conclusion

In this paper, we have introduced a sufficient condition for the impossibility of jamming for three-dimensional, quasistatic, multi-rigid-body systems. This condition applies to manipulator systems moving under position or compliant control and in contact with a passive rigid body (*e.g.*, a workpiece). The condition can be extended to systems with multiple passive rigid bodies and multiple manipulators with kinematic loops.

We are currently running a series of experiments on our prototype dexterous manipulator shown in Figure 5, and are finding that the coefficient of friction can vary wildly for some materials. As a result, the extension of the current theory to handle uncertain friction coefficients is being pursued using the tools of

[2] Recall that Nguyen refers to frictional form closure [2] as "force closure" [5]. However, we reserve the use of the term "force closure" for situations originally identified by Reuleaux [7].

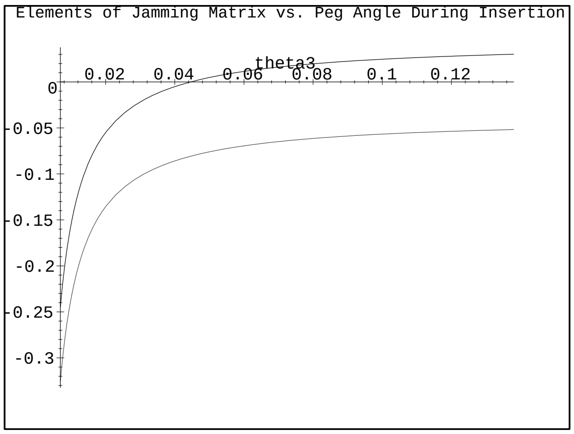

Figure 4: Elements of Jamming Matrix

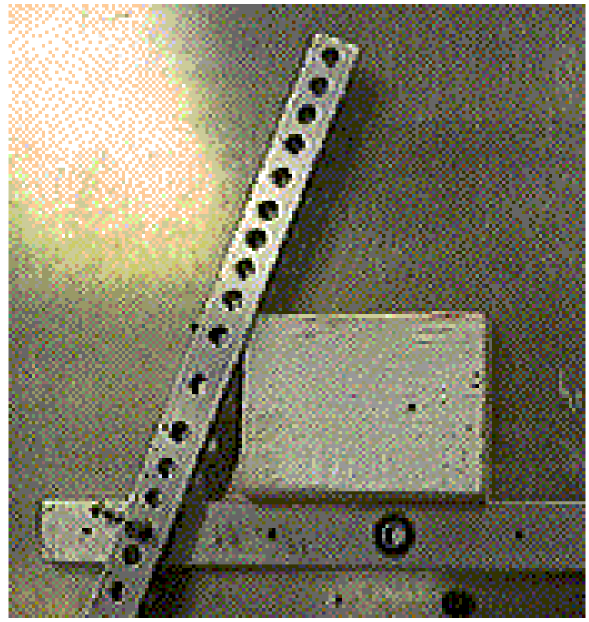

Figure 5: Prototype Planar Dexterous Manipulator

parametric linear programming.

References

[1] M. E. Caine. *The Design of Shape from Motion Constraints.* PhD thesis, MIT Department of Mechanical Engineering, forthcoming.

[2] C. Z. Chammas. Analysis and implementation of robust grasping behaviors. Master's thesis, MIT Department of Mechanical Engineering, May 1990.

[3] B. R. Donald and D. K. Pai. On the motion of compliantly-connected rigid bodies in contact, part II: A system for analyzing designs for assembly. In *Proceedings, IEEE International Conference on Robotics and Automation*, pages 1756–1762, May 1990.

[4] P. E. Dupont and S. P. Yamajako. Jamming and wedging in constrained rigid-body dynamics. In *Proceedings, IEEE International Conference on Robotics and Automation*, pages 2349–2354, May 1994.

[5] V.-D. Nguyen. The synthesis of force closure grasps in the plane. Master's thesis, MIT Department of Mechanical Engineering, September 1985. AI-TR861.

[6] T. Omata. Fingertip positions of a multifingered hand. In *Proceedings, IEEE International Conference on Robotics and Automation*, pages 1562–1567, May 1990.

[7] F. Reuleaux. *The Kinematics of Machinery.* Macmillan, 1876. Republished by Dover, New York, 1963.

[8] S. Simunovic. Force information in assembly processes. In *Proceedings, 5th International Symposium of Industrial Robots*, pages 415–431, September 1975.

[9] J.C. Trinkle, A.O. Farahat, and P.F. Stiller. First-order stability cells of active multi-rigid-body systems. *IEEE Transactions on Robotics and Automation*, 11(4):545–557, August 1995.

[10] J.C. Trinkle and D.C. Zeng. Planar quasistatic motion of a lamina with uncertain contact friction. In *Proceedings, IEEE International Conference on Intelligent Robots and Systems*, pages 1642–1649, 1992.

[11] J.C. Trinkle and D.C. Zeng. Prediction of the quasistatic planar motion of a contacted rigid body. *IEEE Transactions on Robotics and Automation*, 11(2):229–246, April 1995.

[12] D. E. Whitney. Quasi-static assembly of compliantly supported rigid parts. *Journal of Dynamic Systems, Measurement, and Control*, 104:65–77, March 1982.